Ab-initio DFT simulation of electronic and magnetic properties of Tin+1and FeTin clusters

Rachida Haichour (cipcq19bejaia@gmail.com)
Universite Abderrahmane Mira de Bejaia: Universite de Bejaia
Sofiane MAHTOUT
Université de Béjaïa: Universite de Bejaia

Research Article

Keywords: Structural properties, electronic properties, magnetic properties, DFT-GGA, clusters, Fe-Ti

Posted Date: December 29th, 2021

DOI: https://doi.org/10.21203/rs.3.rs-1155624/v1

Abstract

We report a computational investigation of the electronic and magnetic properties of neutral $Ti_{n+1}$and $FeTi_n$ (n=1-10) clusters using ab-initio calculations based on density functional theory (DFT) within the generalized gradient approximation (GGA). The best structures for $Ti_{n+1}$and $FeTi_n$ clusters are planar for size n<5, while from n = 5, they showed a compact three dimensional cage structure. For the best structures of the $FeTi_n$ clusters, the Fe atoms favors the peripheral position with highest coordination with the neighboring Ti atoms. The evolution as a function of the size of the average binding energies (Eb/atom) and HOMO–LUMO gaps of Ti_{n+1} and $FeTi_n$ (n=1-10) clusters are studied. The stability results show that the Ti_{n+1} clusters have relatively higher stability than the $FeTi_n$ cluster with the same size. In addition, the vertical ionization potentials and electron affinities, chemical hardness and atomic magnetic moment of $Ti_{n+1}$and $FeTi_n$ (n=1-10) clusters are also investigated.

1. Introduction

During the last four decades, the semiconductor and transition metal clusters intensively studied because of their specific properties and their great potential use in optoelectronic materials and others nanotechnologies area. The properties of titanium clusters have been investigated because they are interesting for the fine processing and the synthesis of novel materials and the exploration of possibilities of finding novel species and phenomena. Due to the particularity of their properties, the titanium material is applied in many fields especially in medical and different industrial processes. In the literature data, less attention has been allowed to the small titanium clusters. In order to explore and understand the structural, electronic and magnetic behavior of the pure and doped titanium clusters different authors have recently carried out many experimental and theoretical works.

A number of theoretical [1–8, 9] and experimental [10–14] studies about pure Titanium clusters have been reported. They have drawn much attention for their numerous applications in the nano-electronics area [6–8]. In addition, the doping Ti_n clusters with transition-metal atom have been often used to change the chemical and physical properties of the small clusters [6–9, 12, 15–19]. In experimental studies, Lian et al. [10] used the collision induced dissociation for Ti_n^+ (n=2-22) by using a guided beam mass spectrometer. They found that the evolution of the dissociation energy with the size show local important peaks at n=7, 13 and 19.

Sakurai et al.[11] using a TOF mass spectrometry of Ti_n clusters with up to 30 atoms found that Ti_7, Ti_{13}, Ti_{15}, Ti_{19} and Ti_{25} were the magic numbers. With anion photoelectron spectra, Wu et al. [13] show that the 3d band appears at n=8 then widens and evolves towards the bulk band in the charged Ti_n^- (n=3-65) clusters. Using resonant tow-photo ionization technique, Doverstål et al. [14] studied Ti dimer and found a bond length as 1.9429 ± 0. 0013Å. Neukermans et al. [20–21], basing on the photo-fragmentation experiments, investigated the stability of Au_nX^+ clusters doped with a 3d atoms from Sc to Ni and Au_nX_m clusters (X = Sc, Ti, Cr, Fe). Kim et al. [22] studied nanoparticles of Ti-Cr using the electrical wire explosion

of electrode posted metal wires. Koyasu et al. [23] proved, experimentally by using mass and photoelectron spectroscopies the high stability of MSi_{16} clusters while Furuse et al. [24] studied the MSi_{16}^-, MGe_{16}^-, MSn_{16}^- and MPb_{16}^- by experimental and theoretical characterization and they confirmed the exceptional stability for MSi_{16}.

In the theoretical aspect, Anderson [25] investigate with very early Hükel molecular orbital calculations the properties of Ti_{2-6} clusters. Wei et al. [26], by using DFT and LSDA approch investigated the properties of Ti_n (n=2-10) clusters. They found that Ti_7 with good stability is a magic number. Zhao et al. [3] studied the properties of Ti_n (n=2-14, 19 and 55) by using the plane wave ultra-soft pseudopotential method and GGA approach. They found a pentagonal growth models for the clusters and a rapid convergence towards bulk bands for electron density of state. Using GGA, Castro [5] investigated the properties of small Ti_n^- and Ti_n (n= 3-8, and 13) clusters. The structures of small Ti_n (n=2-5) were also studied by Duet al. [4]. Salazar-Vallanueva [27] investigated the structure of Ti_n (n=2-15) clusters and they identified that they are three magic number clusters n= 7, 13 and 15. Lee et al. [28] studied the stability of titanium clusters taking into account the spin polarization and structural distortion. The magnetic properties of Ti_n (n=2-13) clusters have been studied by Medina et al. [29]. By using genetic algorithm, Lazauskas et al. [30] investigate the potential energy surface (PES) for small Ti_n (n = 2–32) clusters. Sun et al. [1] studied by fully self-consistent DFT-based calculation, the evolution as a function of the size the electronic properties of Ti_n (n=2-20). The stabilization mechanism of Ti_n clusters with n=3, 4, 5, 7, 13, 15 and 19 have also investigated by Sun et al. [2]. The same author and their co-workers, have also studied the magnetic and structural properties of $Ti_{12}M$ clusters (M=Sc to Zn) [8] and $Ti_{n-x}Al_x$ (n=2-8, 13, x=0-n) [15], by using the DFT approach. Somme other authors have also interested to the properties titanium clusters such as: Ni_xTi_y ($x+y \leq 5$) [16], Ti_nP (n=1-12) [17], Au_nTi (n=1-9) [18], Ti-Ni clusters [6, 7], $Pt_{x-y}M_y$ (M= Ti, V) [19] and $Ga_nTi_n^{(0,\pm1)}$ (n=1-10) [31].

The purpose of this study is to investigate by using the ab initio and DFT approach the different properties of the small sized titanium clusters doped by iron atom. In the literature data, to our knowledge, there is no studies on the small neutral and iron-doped titanium clusters until now. Therefore, the geometries, stabilities, electronic and magnetic properties of Ti_n and $FeTi_n$ (n = 1-10) clusters will be studied. We hoped that our results will provide powerful guidelines for further studies and would be helpful to understand the effect of the introduction of transition metal impurity on the metallic and semiconducting cages and its properties. The article is organized as follows. In Section 2 we give the theoretical methods and simulation parameters which are used in this study. Presentation and the analysis of the obtained results are presented in Section 3, finally we give the conclusions of this work in Section 4.

2. Method

In this work, all of the calculations on the geometry optimizations of $FeTi_n$ clusters were performed using DFT approach [32] in the generalized gradient approximation (GGA) with the Perdew, Burke and Ernzerhof parameterization (PBE) [33] for the exchange-correlation term, implemented in the SIESTA package [34]. In

order to obtain the best energy structure, a large number of possible initial structures have been considered in geometry optimizations. All geometry optimizations are done with any symmetry constraints. Using the conjugate gradient scheme, the geometries are relaxed without any symmetry constraints. A large supercell with side-length of 40 Å is used to avoid the different interaction between the neighboring systems. The single gamma-point (Γ) was used in the k grid integration. Double zeta basis with polarization functions (DZP) was used for both Fe and Ti species. Self-consistent flied electronic calculations are done with a convergence condition of 10^{-4}a.u. of the total energy. For the geometry optimization, the convergence criteria is 10^{-3} eV/Å for the forces. The validation of this current computational was performed by the calculations tests on Ti_2 and Fe_2 dimers. The obtained results are given in Table 1. It shows the reliability of current computational method to study the small $FeTi_n$ clusters.

Table 1
Comparison of our calculated bond length of Ti_2 and Fe_2 with previous experimental and theoretical values.

Dimer	This work	Theoretical value	Experimental value
Ti_2	2.059	1.98[a], 1.971[b], 1.969[c], 1.951[d] ,1.95[a], 1.944[e]	1.97[f] ,1.945[g] ,1.943[h]
Fe_2	2.126[n]	2.22[i], 2.15[j], 2.10[k], 2.04[l] ,2.003[m]	2.020 ±0.2[n], 1.87[o]

[a] From Ref.[29], [b] From Ref.[15], [c] From Ref.[27], [d] From Ref.[8], [e] From Ref.[1], [f] From Ref.[35], [g] From Ref.[36], [h] From Ref.[14], [i] From Ref. [37], [j] From Ref.[38], [k] From Ref.[39], [l] From Ref.[40], [m] From Ref. [41],[n] From Ref.[42], [o] From Ref.[43],

3. Results And Discussion

3.1. Geometrical structures of pure and Fe doped Ti_n clusters:

In firs time we describe the equilibrium structures of pure titanium clusters. The obtained lowest energy structures and their first close isomers are shown in Fig. 1. Their other physical parameters are given in Table 2. For Ti_2 the dimer with $D_{\infty h}$ symmetry the obtained bond length Ti-Ti is 2.059 Å which is in good agreement with the previous theoretical and experimental values which given in Table 1. For the trimer Ti_3 (a), the ground state isomers is triangular structure with C_{2v} symmetry. The average bond length is obtained to be 2.647 Å and an apex angle of 76.911°. For Ti_5 the geometries exploration of the ground state isomers revel that the rhombus pyramid (C_{4v}) with 2.226 eV/atom is the lowest energy structures. The best energy structure for Ti_6 is a trigonal antiprism (C_{2v}) with 2.536 eV/atom and average bond length Ti-Ti of 2.784 Å. For Ti_7, the caped trigonal antiprism Ti_7(a) with C_1 symmetry is considered as the most stable structure with 2.622 eV/atom. In the case of Ti_8, the regular cubic structure with high symmetry O_h (a) is obtained as the lowest energy structure with average binding energy of 2.554 eV/atom. For Ti_9, the lowest energy isomer is a capped cubic structure Ti_9(a) with average binding energy of 2.808eV/atom and

C_1 symmetry. Bi-capped square antiprism Ti_{10} (a) with symmetry C_s and binding energy of 2.946 eV/atom is found the lowest energy isomers for n=10. Like spherical compact structure with one core atom, bending energy of 3.069 eV/atom and C_1 symmetry obtained as the best structure for Ti_{11}.

Table 2
Point group, binding energy per atom E_b (eV/atom), HOMO-LUMO gap Eg (eV), average bond length a_0(Å), vertical ionization potential VIP (eV), electronic affinity VEA (eV), Chemical hardness η (eV) and atomic magnetic moment μ (μ_B/atom) of Ti_{n+1}(n = 1-10) clusters.

Cluster size (n)	Point group	Eb (eV/atom)	Eg(eV) (eV)	a_0(Å)	VIP(eV)	VEA(eV)	η(eV)	μ (μ_B/atom)
2	$D_{\infty f}$	1.450	0.022	2.059	5.203	0.050	5.152	3.0
3	(a) C_{2v}	1.883	0.555	2.647	5.221	0.682	4.539	33
	(b) D_{3h}	1.741	0.843	2.383	5.257	0.053	5.204	2.7
	(c) $D_{\infty f}$	1.696	0.238	2.517	5.261	0.393	4.868	3.3
4	(a) C_s	2.029	0.808	2.793	5.118	0.027	5.090	2.5
	(b) D_{2h}	2.024	0.678	2.840	5.622	0.532	5.090	2.5
	(c) D_{4h}	1.859	0.284	2.458	4.436	0.709	3.728	2.6
5	(a) C_{4v}	2.226	0.459	2.640	5.763	0.203	5.559	2.0
	(b) C_{4v}	2.225	0.459	2.641	5.756	0.196	5.560	2.0
	(c) C_1	2.197	0.591	2.794	6.643	1.138	5.505	2.0
	(d) D_{3h}	2.152	0.558	2.632	5.666	0.172	5.493	1.2
6	(a) C_{2v}	2.536	0.391	2.784	5.514	0.321	5.192	2.0
	(b) D_{2h}	2.532	0.355	2.748	7.917	2.109	5.808	2.3
	(c) O_h	2.513	0.460	2.758	7.826	2.036	5.790	2.3
	(d) C_1	2.493	0.418	2.883	7.826	2.148	5.678	1.7
7	(a) C_1	2.622	0.331	2.857	6.508	0.609	5.899	1.7
	(b) D_{5h}	2.592	0.410	2.774	7.434	1.537	5.896	1.1
	(c) D_{2h}	2.393	0.529	2.902	7.412	1.431	5.981	2.0
	(d) C_1	2.371	0.382	2.787	7.390	1.991	5.400	2.9
8	(a) O_h	2.554	0.654	2.690	6.718	1.123	5.596	2.7
	(b) C_1	2.453	0.322	2.813	8.730	3.582	5.148	3.2

Cluster size (n)	Point group	Eb (eV/atom)	Eg(eV) (eV)	a_0(Å)	VIP(eV)	VEA(eV)	η(eV)	μ (μ_B/atom)
	(c) C_s	2.444	0.493	2.881	7.613	2.037	5.576	2.8
	(d) C_2	2.439	0.549	2.891	8.449	2.881	5.568	3.0
9	(a) C_1	2.808	0.403	2.828	8.804	3.322	5.482	2.2
	(b) C_s	2.788	0.239	2.875	8.824	3.078	5.746	2.0
	(c) C_1	2.785	0.343	2.930	10.342	5.081	5.261	2.4
	(d) C_s	2.774	0.346	2.843	9.078	3.425	5.653	2.4
10	(a) C_s	2.946	0.371	2.848	14.031	8.486	5.546	3.3
	(b) C_1	2.888	0.261	2.893	9.494	4.077	5.417	2.4
	(c) C_1	2.825	0.293	2.863	10.269	5.121	5.148	2.8
	(d)D_{4h}	2.728	0.547	2.794	8.696	2.740	5.841	2.8
	(a) C_1	3.069	0.255	2.859	13.117	7.259	5.857	2.0
11	(b) C_1	2.996	0.356	2.866	10.878	4.926	5.951	1.8
	(c) D_{4h}	2.958	0.251	2.864	11.418	5.509	5.909	2.2
	(d) C_1	2.895	0.212	2.908	11.371	5.978	5.393	2.9

For doped $FeTi_n$ clusters, the most stables structures and their corresponding isomers are shown in Fig. 2. For FeTi dimer, the bond length Fe-Ti is 2.941 Å much larger than their corresponding Ti_2 dimer. As in the case Ti_3 cluster, the best isomer of $FeTi_2$ is triangular structure with Fe-Ti bond length of 2.887 Å and C_{2v} symmetry. For $FeTi_3$, the lowest energy structure is triangular based pyramid with binding energy 1.752 eV/atom and C_{3v} symmetry. In the case of $FeTi_4$ cluster, a bi-capped tetrahedron with binding energy of 1.949 eV/atom and C_{3v} for symmetry is find as the best isomer. For $FeTi_5$, the best isomer is a distorted bi-capped tetragonal structure with 2.322 eV/atom and C_s symmetry. In the case of $FeTi_6$, our calculations show that the tri-capped triangular base pyramid structure is the most stable one with Cs symmetry. The Fe atom is located at the surface of the cluster cage and highly coordinated to all of the other Ti atoms in the system. The lowest energy isomer for $FeTi_7$ is a by the composition of a rectangular and tetragonal bi-capped structures with O_h symmetry and binding energy of 2.576 eV/atom. This structure is only 0.041 eV/atom more stable than their first isomer $FeTi_7$ (b) with D_{4h} symmetry. For $FeTi_8$, the most stable structure is composed by two distorted tetragonal based pyramid with binding energy of 2.786 eV/atom

and high symmetry D_{2d}. The lowest energy isomer for $FeTi_9$ is a like-spherical compact structure with Fe atom occupied a peripheral position (C_1) and binding energy of 2.792 eV/atom. In the case of $FeTi_{10}$, the lowest energy structure is a Fe centered a bi-capped cubic structure with 2.925 eV/atom and high symmetry D_{4h}. The centered position and the high coordination number of Fe atom can be the origin of the good stability of this structure. As we see from the Table 2 and Table 3 that, the average bond length of both Ti_{n+1} and $FeTi_n$ (n=1-10) show an increasing tendency as the cluster size increase. In addition, in the most of the best structure of $FeTi_n$ clusters, the Fe atom occupies the highest coordinated site in the clusters and this behavior increase as the size of cluster increase. These two geometrical parameters can have direct consequences on hybridization between Fe and Ti atoms. It turns out a considerable changing of the clusters electronic and magnetic properties.

Table 3
Point group, binding energy per atom E_b (eV/atom), HOMO-LUMO gap E_g (eV), average bond length a_0(Å), vertical ionization potential VIP (eV), electronic affinity VEA (eV), Chemical hardness η (eV) and atomic magnetic moment μ (μ_B/atom) of $FeTi_n$ (n = 1-10) clusters.

Cluster size (n)	Point group	E_b (eV/atom)	E_g (eV)	a_0 (Å)		VIP(eV)	VEA(eV)	η(eV)	μ (μ_B/atom)
				Ti-Ti	Ti- Fe				
1	$C_{\infty v}$	0.868	0.991	/	2.941	6.844	0.776	6.067	3.7
2	(a) C_{2v}	1.236	0.320	/	2.887	9.580	1.452	8.128	3.3
	(b) $D_{\infty f}$	1.101	0.655	/	2.458	8.832	0.334	8.497	3.3
3	(a) C_{3v}	1.752	0.458	2.363	2.706	5.929	0.226	5.703	2.0
	(b) C_{2v}	1.585	0.505	2.448	2.760	6.981	1.412	5.570	3.0
	(c) C_{2v}	1.551	0.468	2.411	2.641	5.173	0.535	4.638	2.5
	(d) C_{2v}	1.550	0.467	2.415	2.641	5.132	0.517	4.616	2.5
4	(a) C_{3v}	1.949	0.640	2.538	2.694	5.706	0.092	5.614	1.6
	(b) C_{2v}	1.877	0.875	2.742	2.687	5.555	0.301	5.254	2.4
5	(a) C_s	2.322	0.598	2.703	2.854	7.853	1.484	6.369	2.3
	(b) C_2	2.309	0.510	2.771	2.842	7.252	1.530	5.723	2.7
	(c) C_2	2.292	0.517	2.748	2.812	7.181	1.434	5.748	2.7
	(d) C_1	2.081	0.576	2.777	2.839	8.211	4.344	3.866	3.0
6	(a) C_s	2.437	0.214	2.877	2.831	12.153	6.213	5.940	2.3
	(b) C_1	2.406	0.444	2.860	2.823	8.324	3.117	5.207	2.3
	(c) C_{5v}	2.345	0.293	2.754	2.727	7.351	1.783	5.568	2.0
	(d) D_{6h}	2.336	0.436	2.696	2.696	8.340	2.141	6.199	2.0

Cluster size (n)	Point group	E_b (eV/atom)	E_g (eV)	a_0 (Å)		VIP(eV)	VEA(eV)	η(eV)	μ (μ_B/atom)
				Ti-Ti	Ti- Fe				
7	(a) O_h	2.576	0.543	2.785	2.890	7.697	3.182	4.515	2.5
	(b) D_{4h}	2.535	0.435	2.806	2.904	19.145	8.724	10.421	3.0
	(c) C_1	2.260	0.663	2.858	2.853	16.739	6.787	9.952	3.0
	(d) C_s	2.222	0.372	2.725	2.656	6.771	2.271	4.500	2.5
8	(a) D_{2d}	2.786	0.243	2.789	2.494	8.406	2.905	5.501	2.2
	(b) C_1	2.732	0.389	2.842	2.772	7.597	2.454	5.143	1.8
	(c) C_1	2.603	0.353	2.799	2.329	10.231	4.826	5.406	2.9
	(d)C_{4v}	2.468	0.384	2.679	2.792	6.672	1.226	5.446	2.4
9	(a) C_1	2.792	0.251	2.894	2.329	12.562	6.936	5.626	2.4
	(b) C_1	2.786	0.358	2.828	2.856	10.057	5.032	5.025	2.4
	(c) C_1	2.746	0.192	2.828	2.329	9.786	3.844	5.941	1.8
	(d) C_1	2.732	0.164	2.809	2.950	9.768	4.435	5.334	2.8
	(a) D_{4h}	2.925	0.178	2.871	2.856	10.209	4.918	5.291	2.5
10	(b) C_1	2.868	0.374	2.847	2.856	10.481	5.120	5.361	1.6
	(c) C_1	2.855	0.291	2.855	2.856	11.641	7.634	4.007	2.2
	(d) C_1	2.847	0.318	2.905	2.798	13.246	7.325	5.921	2.0

3.2. Relative stability and electronic properties:

In this section, the relative stability of the Ti_{n+1} and $FeTi_n$ (n = 1-10) clusters will be analyzed and discussed by using the different values of the averaged binding energy, second-order energy difference, HOMO-LUMO gaps (the difference in energy between the highest occupied molecular orbital (HOMO) and the lowest unoccupied molecular orbital (LUMO)), the vertical ionization potential (VIP) and the vertical electron affinity (VEA).

The averaged binding energy (Eb/atom) is useful for quantity to study the stability of small clusters. This parameter can be calculated for Ti_{n+1} and $FeTi_n$ as follows:

$$E_b\left[Ti_{n+1}\right] = [(n+1)E(Ti) - E(Ti_{(n+1)})]/(n+1) \quad (1), (1)$$

$$E_b\left[FeTi_n\right] = \left[E(Fe) + nE(Ti) - E\left(FeTi_n\right)\right]/(n+1)$$

2

,

Where $E_b\left(Ti_{n+1}\right)$ and $E_b\left(FeTi_n\right)$ represent, respectively, the total energy of Ti_{n+1} and $FeTi_n$ clusters, and E(Ti) and E(Fe) are the single energies for frees Ti and Fe atoms. The obtained values of binding energies for two systems are given in Tables 2 and 3. Their evolutions as a function of the size for the most stable clusters of each size are plotted in Fig. 3. We note the monotonically increasing of binding energy with the increasing of cluster size, which means that these clusters will get energy during their growth. Since, the overall stability (binding energy) is supposed to increase and reach the bulk value of titanium, which is experimentally reported to be 4.85 eV [44], where a cluster requires up a very large number of atoms [45]. We can also see, that the binding energy for Ti_{n+1} clusters are larger than those of $FeTi_n$. Which means that the doping Fe atom does not enhance the stability of host Ti_n clusters at small size. However, we observe, for n=7 and n= 8, very close equal values of the binding energy of $FeTi_n$ cluster and those of corresponding pure Ti_{n+1}. We notice local peaks in the curve of Ti_{n+1} at size n=2 and n=6 implying that Ti_3 and Ti_7 are more stable than their neighbors where Ti_7 is reported as a magic number in the previous studies [1, 7, 11]. In addition, $FeTi_3$, $FeTi_5$ and $FeTi_8$ show high stabilities compared to their other neighboring clusters.

The second-order energy difference (ΔE_2) is calculated for the best structures of each size by using:

$$\Delta_2 E\left(Ti_{n+1}\right) = E\left(Ti_{n+2}\right) + E\left(Ti_n\right) - 2E\left(Ti_{n+1}\right)$$

3

,

$$\Delta_2 E\left(FeTi_n\right) = E\left(FeTi_{n+1}\right) + E\left(FeTi_{n-1}\right) - 2E\left(FeTi_n\right)$$

4

,

Where E represents the total energy for corresponding cluster. In cluster sciences, this quantity Δ_2E is an interesting quantity that reflects the relative stability of clusters. The systems with positive values are more stable than those with negative values of $\Delta_2 E$. The calculated value of $\Delta_2 E$ for the most stable Ti_{n+1} and $FeTi_n$ clusters are plotted in Fig. 4. We notice the pronounced positive value of $\Delta_2 E$ at Ti_7 for pure Ti_{n+1} indicating that this cluster has a special stability what has already well- mentioned at binding energy Fig. 3. In addition, this number refers to the magic number cluster observed during the experimental studies [10, 11]. Although HOMO-LUMO gap curve shows a dip at this size, meaning that the enhanced stability is due to geometric effects instead of electronic effects [1, 46, 47]. As we can see, $FeTi_6$ is less stable than Ti_7 but a prominent maximum is found for $FeTi_3$, $FeTi_5$ and $FeTi_8$ indicating that they are more stable than the others clusters.

The measurement of the HOMO-LUMO gap, which depends on the eigenvalues of the HOMO and LUMO energy levels, is important to characterize the electronic properties in clusters. Its knowledge is useful to examine the chemical reactivity and the chemical stability of clusters. A large HOMO-LUMO energy gap indicates a weaker chemical reactivity and high strength required perturbing the electronic structure and bigger HOMO-LUMO gap signifies a higher stability. Clusters with very large gap have a very low chemical reactivity and a high chemical stability [8, 48]. In Fig. 5, the obtained HOMO-LUMO gaps are plotted as a function of cluster size for pure Ti_{n+1} and doped $FeTi_n$ (n=1-11). It is interesting to note that the obtained HOMO-LUMO gaps varies between 0.164-0.991 eV for $FeTi_n$ clusters and 0.022-0.843 for Ti_{n+1} clusters, which indicate that the metallic behavior can be observed for these two systems. Thus, these clusters can be used in catalytic reactions applications. The behaviors show a general decrease of the HOMO-LUMO gap as the cluster size increase for both Ti_{n+1} and $FeTi_n$ clusters. Also, the $FeTi_n$ clusters have generally a smallest HOMO-LUMO gap comparing to a pure Ti_{n+1}. Indicating that the Fe doping atom weakens the chemical stability and enhances the metallic behavior for the $FeTi_n$ clusters. We observe that the clusters FeTi and Ti_4 have the largest value of HOMO-LUMO gaps suggesting that these clusters have a higher chemical stability and a smaller chemical reactivity than their neighbors.

In cluster physics, VIP and VEA are considered as important measurement that can reflect the chemical stability of the small clusters. The VIP is calculated by the difference in energy between the cationic and neutral clusters with the same geometry of the neutral structure and the VEA is the energy difference between the neutral and anionic cluster with the same geometry of the neutral structure. In addition, these two parameters are instructive to examine another quantity, which is the global chemical hardness. The higher value of VIP indicates that they need more energy for the cluster to lose one electron and the smaller value of VEA indicates that the cluster is more difficult to accept an electron, meanwhile the neutral cluster is high chemically stable.

The VIP and VEA are defined for pure and doped titanium clusters as:

$$VIP = E\left(Ti_{n+1}^{+}\right) - E\left(Ti_{n+1}\right)$$

5
,

$$VEA = E\left(Ti_{n+1}\right) - E\left(Ti_{n+1}^{-}\right)$$

6
,

$$VIP = E\left(FeTi_{n}^{+}\right) - E\left(FeTi_{n}\right)$$

7
,

$$VEA = E\left(FeTi_{n}\right) - E\left(FeTi_{n}^{-}\right)$$

8
,

E is the total energy of the considered neutral cluster while $E\left(Ti_{n+1}^{+}\right)$ / $E\left(FeTi_{n}^{+}\right)$ and $E\left(Ti_{n+1}^{-}\right)$ / $E\left(FeTi_{n}^{-}\right)$ are, respectively, the total energies of the cationic and anionic clusters. The obtained results of VIP and VEA are given in Table 2 and 3, plotted, respectively, in Fig. 6 and Fig. 7.As we see from figure (06), the VIP increase monotically for pure titanium clusters and show an oscillating behavior with a trend to increase with increasing size for iron doped titanium clusters. In addition, the VIP exhibits obvious odd-even oscillations from the size 2 to 7. From Fig. 07, we observe that the VEA increases with the increasing size n with an obvious increasing from n=6. The largest values of VEA are in general observed for the large sized clusters, which mean that we need more energy to add an electron to the systems, indicating the growing of their stability. Among the Ti_{n+1} and $FeTi_n$ clusters, $FeTi_6$, $FeTi_9$ and $FeTi_{10}$ show a pronounced peak for VIP and VEA parameters which indicates their high stability compared to the neighboring clusters.

By using the obtained values of VIP and VEA, we investigated the chemical hardness (η) of Ti_{n+1} and $FeTi_n$ clusters. Chemical hardness is an important parameter that characterizes the resistance to charge transfer and the stability of clusters. A large value of chemical hardness corresponds to a less reactivity and a higher stability. According to the maximum hardness principles (PMH) [49], the chemical hardness is calculated by:

$$\eta = VIP - VEA$$

9
,

The calculated values for the most stables structures of both Ti_{n+1} and $FeTi_n$ clusters are given in Tables 2 and 3, and shown in Fig. 8. As we can see from the figure, the chemical hardness has a decreasing evolution with the increasing of the size for $FeTi_n$ clusters. Except for n=7 and 10 the chemical hardness of $FeTi_n$ clusters are higher than the pure Ti_{n+1} clusters with the same number of atoms. Through the PMH of chemical hardness, this result indicates that the doped clusters with higher value of chemical hardness are more stable than the corresponding pure clusters. Among the observed values of η, a pronounced peak are observed for $FeTi_2$ and $FeTi_5$ clusters, which indicate their very less chemical reactivity.

3.3. Magnetic properties:

The magnetic properties of Ti_{n+1} and $FeTi_n$ are studied under the spin polarized DFT calculations. These magnetic properties are studied by the evaluation of the total spin magnetic moment, which is calculated by the difference between the Mullikan charge populations for the electrons with spin up and the electrons with spin down. The obtained average atomic of spin magnetic moments (SMM) of the two systems are given in Tables 2 and 3 and presented Fig. 9. We observe the same variance tendency for both pure Ti_{n+1} and $FeTi_n$ clusters. The average SSM for the two systems decrease with the increase of the size until n=5 for $FeTi_n$ and n=7 for Ti_n clusters. From these sizes, the average SSM for the two systems show an increasing tendency with an oscillating behavior with the increasing of the size. As reported in the previous studies, the bulk titanium is nonmagnetic, but the small Ti_n clusters have significant magnetic moment and it is sensitive to their structures and geometries [7, 17, 18, 26, 29].The same behavior is observed in our results. The FeTi dimer with 3.7 μ_B has the largest average atomic magnetic moment. This is maybe correlated to its linear structure with a long average bond length. For pure Ti_{n+1}, we notice a local peak at n =2 and 9 with 3.3 μ_B which are the highest in all clusters.

In order to understand the relation between the magnetic behavior and structural properties of Ti_{n+1} and $FeTi_n$ clusters, we represent in Fig. 10 the evolution of the average interatomic distances a_0(Ti-Ti) and a_0(Fe-Ti) as a function of cluster size. High differences between a_0(Ti-Ti) and a_0(Fe-Ti) are observed for very small ($n \leq 2$) and large ($n \geq 8$) size of clusters. For these clusters, large values of total spin magnetic moment are observed. Between n=2 and n=8, where the difference between the a_0(Ti-Ti) and a_0(Fe-Ti) is small, the total spin magnetic moment shows reduced values. This result constitutes a direct relationship between the magnetic and structural properties.

To understand the origin of average SMM of Ti_{n+1} and $FeTi_n$ clusters and to evaluate the contribution of different valence orbital (s and d) of the Fe and Ti components, we explore the total and partial densities of states for some low energy structures of the two systems. The obtained results for Ti_3, Ti_6, $FeTi_1$, $FeTi_2$, and $FeTi_4$ clusters are shown in Fig. 11. The spin up densities is plotted as positive and the spin down as negative. From this figure, we can clearly see that the 3d states of Ti and Fe atoms play an important contribution in the determination of the magnetic behavior of the Ti_n and $FeTi_n$ clusters. The 4s states of Ti and Fe atoms contribute little and almost negligible in the $FeTi_n$ systems.

Conclusion

In this work, we have systematically investigate the properties of small Ti_{n+1} and $FeTi_n$ (n=1-10) clusters by using DFT-GGA with PBE parameterization for the exchange-correlation functional calculations. In the doped $FeTi_n$ clusters, the Fe atom occupies preferentially the position near or at the surface is the most favorable geometries. The geometrical structures, stabilities, electronic and magnetic properties of small Ti_{n+1} and $FeTi_n$ are calculated and discussed. The geometric optimizations of Ti_{n+1} clusters show that for each cluster size, multiple isomers and new structures in addition to other structures obtained in the previous studies. The analyses of the binding energies and second-order energies differences show enhanced stability of $FeTi_{3,}$ $FeTi_5$ and $FeTi_8$ clusters. From the HOMO-LUMO gaps, we found that the FeTi and Ti_4 clusters possess a high chemical stability. The average SSM for the two systems depend on the size of $FeTi_n$ and n=7 for Ti_n clusters. The VIP and VEA calculations analysis show that the clusters with large size exhibit high metallic character. Consequently, they will liberate more energy when they gains one electron. The chemical hardness shows that the clusters with small size are less reactive and more stable. PDOS analysis reveal that high value of the average total spin magnetic moment for Ti_{n+1} and $FeTi_n$ clusters is due to the contribution of the valence orbitals with a large domination of 3d states of Ti and Fe atoms. Finally, we hope that these results will serve as a basic resource for further theoretical and experimental research work on new nanoscale materials.

Declarations

Funding:

This work was supported by the open research fund of the “General Direction of Research and Technological Development DGRSDT” of the “Ministry of Higher Education and Scientific Research” and the Exact Sciences Faculty of Bejaia University, Algeria.

Competing Interests:

Authors S. Mahtout and R. Haichour declare they have no financial interests.

Author Contributions:

All authors contributed to the study conception and design. R. Haichour and S. Mahtout performed the simulation, the calculations of different properties and their analysis. S. Mahtout wrote the first draft of the manuscript and all authors commented on previous versions of the manuscript. All authors read and approved the final manuscript.

Code availability:

We used the free code SIESTA for all calculations reported in this study.

Data Availability:

The datasets generated during the current study are available from the corresponding author on reasonable request.

References

1. Sun H, Ren Y, Wu Z, Xu N (2015) Density functional calculation of the growth, electronic and bonding properties of titanium clusters Ti_n (n = 2–20). Comp Theo Chem 1062: 74–83. https://doi.org/10.1016/j.comptc.2015.03.021
2. Sun H, Ren Y, Hao Y, WU Z, Xu N (2015) The stabilization mechanism of titanium cluster. J Phys Chem Solid 80: 105–111. https://doi.org/10.1016/j.jpcs.2015.01.006
3. Zhao J, Qiu Q, Wang B, Wang B, Wang J, Wang G (2001) Geometric and electronic properties of titanium clusters studied by ultrasoft pseudopotential. Solid State Com 118: 157–161. https://doi.org/10.1016/S0038-1098(01)00044-8
4. Du J, Wang H, Jiang G (2007) Structures of the small Ti_n (n=2-5) clusters: A DFT study. J Mol Struct: THEOCHEM 817: 47–53. https://doi.org/10.1016/j.theochem.2007.04.018
5. Castro M, Liu S, Zhai H J, Wang LS (2003) Structural and electronic proprieties of small titanium clusters: A density functional theory and anion photoelectron spectroscopy. J Chem Phys 118: 2116–2123. https://doi.org/10.1063/1.1532000
6. Verkhovtsev AV,Sushko GB, Yakubovich AV, Solov'yov AV (2013) Benchmarking of classical force fields by ab initio calculations of atomic clusters: Ti and Ni–Ti case. Comp Theo Chem 1021: 101–108. https://doi.org/10.1016/j.comptc.2013.06.034
7. Verkhovtsev AV, Hanauske M, Yakubovich AV, Solov'yov AV (2013) Characterization of small pure and Ni-doped titanium clusters: Ab initio versus classical approaches. Comp Mat Sci 76: 80–88. https://doi.org/10.1016/j.commatsci.2013.03.017
8. Sun H, Xu N (2016) Structural and magnetic properties of $Ti_{12}M$ clusters (M=Sc to Zn). J Phys Chem Solid 99: 92–99. https://doi.org/10.1016/j.jpcs.2016.08.010
9. Hurtado RB, Cortez-Valadez M, Gámez-Corrales R, Flores-Acosta M (2018) Structural and vibrational properties of gold-doped titanium clusters: A first-principles study. Comp Theo Chem 1124: 32–38. https://doi.org/10.1016/j.comptc.2017.12.008
10. Lian L, Su CX, Armentrout PB (1992) Collision-induced dissociation of Ti_n^-(n=2-22) with Xe: bond energies, geometric structures, and dissociation pathways. J Chem Phys 97: 4084–4093. https://doi.org/10.1063/1.463913
11. Sakurai M, Watanabe K, Sumiyama K, Suzuki KJ (1999) Magic numbers in transition metal (Fe, Ti, Zr, Nb, and Ta) clusters observed by time-of-flight mass spectrometry. J Chem Phys111: 235–244. https://doi.org/10.1063/1.479268

12. Liu SR, Zhai HJ, Castro M, Wang LS (2003) Photoelectron spectroscopy of Ti_n^- clusters (n = 1 - 130). J Chem Phys118: 2108–2115. https://doi.org/10.1063/1.1531999
13. Wu H, Desai SR, Wang LS (1996) Electronic Structure of Small Titanium Clusters: Emergence and Evolution of the 3^d Band. Phys Rev Lett76: 212–215. https://doi.org/10.1103/PhysRevLett.76.212
14. Doverstål M, Karlsson L, Lindgren B, Sassenberg U (1997) The $^3\Delta_u - X^3\Delta_g$ band system of jet-cooled Ti_2, Chem Phys Lett 270: 273–277. https://doi.org/10.1016/S0009-2614(97)00364-3
15. Sun H, Zhang W, Xu N (2018) Density functional calculation of structural and electronic properties of Ti_n-xAlx (n =2-8, 13, x=0-n) clusters. J Chem Phys118: 126–136. https://doi.org/10.1016/j.jpcs.2018.01.029
16. Venkataramanan NS (2008) Structures of small Ni_xTi_y ($x + y \leq 5$) clusters: A DFT study. J Mol Struct: THEOCHEM 856: 9–15. https://doi.org/10.1016/j.theochem.2008.01.012
17. Wang H, Hu N, Tao DJ, Lu ZH, Nie J, Chen XS (2011) Structural and electronic properties of phosphorus-doped titanium clusters: A DFT study. Comp. Theo. Chem 977: 50–54. https://doi.org/10.1016/j.comptc.2011.09.007
18. Dong D, Ben-Xia Z, Hui W, Quan D (2013) Geometries, stabilities and magnetic properties of Au_nTi (n = 1–9) clusters: A density functional study. Comp. Theo Chem 1025: 67–73. https://doi.org/10.1016/j.comptc.2013.09.022
19. Jenning PC, Johnston RL (2013) Structures of small Ti- and V-doped Pt clusters: A GA-DFT study. Comp. Theo. Chem1021: 91–100. https://doi.org/10.1016/j.comptc.2013.06.033
20. Neukermans S, Janssens E, Tanaka H, Silverans RE, Lievens P (2003) Element and Size-Dependent Electron Delocalization in Au_NX+ Clusters (X=Sc, Ti, V, Cr, Mn, Fe, Co, Ni). Phys Rev Lett 90: 033401.1. https://doi.org/10.1103/PhysRevLett.90
21. Janssens E, Tanaka H, Neukermans S, Silverans RE, Lievens P (2004) Electron delocalization in Au_NX_M (X=Sc, Ti, Cr, Fe) clusters: A density functional theory and photofragmentation study. Phys Rev B 69: 085402. https://doi.org/10.1103/PhysRevB.69.085402
22. Kim W, Park J, Suh C, Cho S, Lee S (2009) Ti-Cr nanoparticles prepared by electrical wire explosion. Mater Trans 50: 2344–2346. https://doi.org/10.2320/matertrans.M2009190
23. Koyasu K, Akutsu M, Mitsui M, Nakajima A (2005) Selective Formation of MSi_{16} (M = Sc, Ti, and V). J Am Chem Soc 127: 4998–4999. https://doi.org/10.1021/ja045380t
24. Furuse S, Koyasu K, Atobe J, Nakajima A (2008) Experimental and theoretical characterization of MSi_{16}^-, MGe_{16}^-, MSn_{16}^- and MPb_{16}^- (M=Ti, Zr, and Hf): The role of cage aromaticity. J Chem Phys 129: 064311. https://doi.org/10.1063/1.2966005
25. Anderson A (1976) Structures binding energies, and charge distributions for two to six atom Ti, Cr, Fe, and Ni clusters and their relationship to nucleation and cluster catalysis. J Chem Phys 64: 4046–4055. https://doi.org/10.1063/1.432013
26. Wei SH, Zeng Z, You JQ, Yan XH, Gong XG (2000) A density functional study of small titanium clusters. J Chem Phys113: 11127–11133. https://doi.org/10.1063/1.1319646

27. Salazar-Villanueva M, Tejeda PHH, Pal U, Rivas-Silva JF, Rodríguez Mora JI, Ascencio JA (2006) Stable Ti_n (n = 2-15) Clusters and Their Geometries: DFT Calculations. J Phys Chem A 110: 10274–10278. https://doi.org/10.1021/jp061332e
28. Lee B, Lee GW (2007) Comparative study of Ti and Ni clusters from first principles. J Chem Phys127: 164316–163420. https://doi.org/10.1063/1.2800026
29. Medina J, De Coss R, Tapia A, Canto G (2010) Structural, energetic and magnetic properties of small Ti_n (n = 2–13) clusters: a density functional study. Eur Phys B 76: 427–433. https://doi.org/10.1140/epjb/e2010-00214-3
30. Lazauskas T, Sokol AA, Buckeridge J, Catlow CRA, Escher SGET, Farrow MR, Mora-Fonz D, Blum VW, Phaahla TM, Chauke HR, Ngoepe PE, Woodley SM (2018) Thermodynamically accessible titanium clusters Ti_N, N = 2–32, Phys Chem Chem Phys 20: 13962–13973.DOI: 10.1039/C8CP00406D
31. Shi S, Liu Y, Den B, Zhang C, Jiang G (2014) Geometries, stabilities, and electronic properties of small $Ga_nTi^{(0,\pm1)}$ (n = 1–10) clusters studied by density functional theory. Comp. Mat Sci 95: 476–483. https://doi.org/10.1016/j.commatsci.2014.07.059
32. Ordejón P, Artacho E, Soler JM (1996) Self-consistent order-N density-functional calculations for very large systems. Phys Rev B 53: R10441-R10444. https://doi.org/10.1103/PhysRevB.53.R10441
33. Perdew JP, Burke K, Ernzerhof M (1996) Generalized gradient approximation made simple. Phys Rev Lett 77: 3865–3868. https://doi.org/10.1103/PhysRevLett.77.3865
34. Soler JM, Artacho E, Gale JD, García A, Junquera J, Ordejón P, Sánchez-Portal D (2002) The SIESTA method for ab initio order-N materials simulation. J Phys Cond Matt 14: 2745–2766. https://doi.org/10.1088/0953-8984/14/11/302
35. Morse MD (1986) Clusters of transition-metal atoms. J Chem Rev 86: 1049–1109 https://doi.org/10.1021/cr00076a005
36. Russon LM, Heldecke SA, Birke MK, Conceicao J, Morse MD, Armentrout PB (1994) Photodissociation measurements of band dissociation energies: Ti_2^+; V_2^+; and CO_3^+. J Chem Phys 100: 4747–4755. https://doi.org/10.1063/1.466265
37. Cheng HP, Ellis DE (1991) Electronic structure, binding energies, and interaction potentials of transition metal clusters. J Chem Phys 94: 3735–3747. https://doi.org/10.1063/1.459745
38. Nakazawa T, Igarashi T, Tsuru T, Kaji Y(2009) Ab initio calculations of Fe-Ni clusters. Comp Mat Sci 46: 367–375. https://doi.org/10.1016/j.commatsci.2009.03.012
39. Harris J, Jones RO (1979) Density functional theory and molecular bonding. III. Iron-series dimers. J Chem Phys 70: 830–841. https://doi.org/10.1063/1.437516
40. Liang XQ, Deng XJ, Lu SJ, Huang XM, Zhao JJ, Xu HG, Zheng WJ, Zeng XC (2017) Probing structural, electronic, and magnetic properties of iron-doped semiconductor clusters Fe_2 $Ge_n^{-1/0}$ (n=3–12) via Joint photoelectron spectroscopy and density functional study. J Phys Chem C.121: 7037–7046. https://doi.org/10.1021/acs.jpcc.7b00943

41. Cervantes-Salguero K, Seminario JM (2012) Structure and energetics of small iron clusters. J Mol Mod 18: 4043–4052. https://doi.org/10.1007/s00894-012-1395-2
42. Purdum H, Montano PA, Shenoy GK, Morrison T (1982) Extended-x-ray-absorption-fine-structure study of small Fe molecules isolated in solid neon. Phys Rev B 25: 4412–4417. https://doi.org/10.1103/PhysRevB.25.4412
43. Montano PA, Shenoy GK (1980) EXAFS study of iron monomers and dimers isolated in solid argon. Sol Stat Comm 35: 53–56. https://doi.org/10.1016/0038-1098(80)90769-3
44. Philipsen PHT, Baerends EJ (1996) Cohesive energy of 3d transition metals: Density functional theory atomic and bulk calculations. Phys Rev B 54: 5326–5333. https://doi.org/10.1103/PhysRevB.54.5326
45. Alonso JA (2000) Electronic and Atomic Structure, and Magnetism of Transition-Metal Clusters. Chem Rev 100: 637–678. https://doi.org/10.1021/cr980391o
46. Reveles JU, Sen P, Pradhan K, Roy DR, Khanna SN (2010) Effect of Electronic and Geometric Shell Closures on the Stability of Neutral and Anionic $TiNa_n$ (n = 1–13) Clusters. J Phys Chem C 114: 10739–10744. https://doi.org/10.1021/jp101757n
47. Chauhan V, Singh A, Majumder C, Sen P (2014) Structural, electronic and magnetic properties of binary transition metal aluminum clusters: absence of electronic shell structure. J Phys Cond. Matt 26: 015006.1 https://doi.org/10.1088/0953-8984/26/1/015006
48. Siouani C, Mahtout S, Rabilloud F (2019) Structure, stability, and electronic properties of niobium-germanium and tantalum-germanium clusters. J Mol Mod 25: 113. https://doi.org/10.1007/s00894-019-3988-5. Mahtout S, Siouani C, Rabilloud F (2018) Growth Behavior and Electronic Structure of Noble Metal-Doped Germanium Clusters. J Phys Chem A 122: 662-677. https://doi.org/10.1021/acs.jpca.7b09887
49. Parr RG, Yang W (1989) Density Functional Theory of Atoms and Molecules. Oxford University Press, New York 1989. https://doi.org/10.1007/978-94-009-9027-2_2

Figures

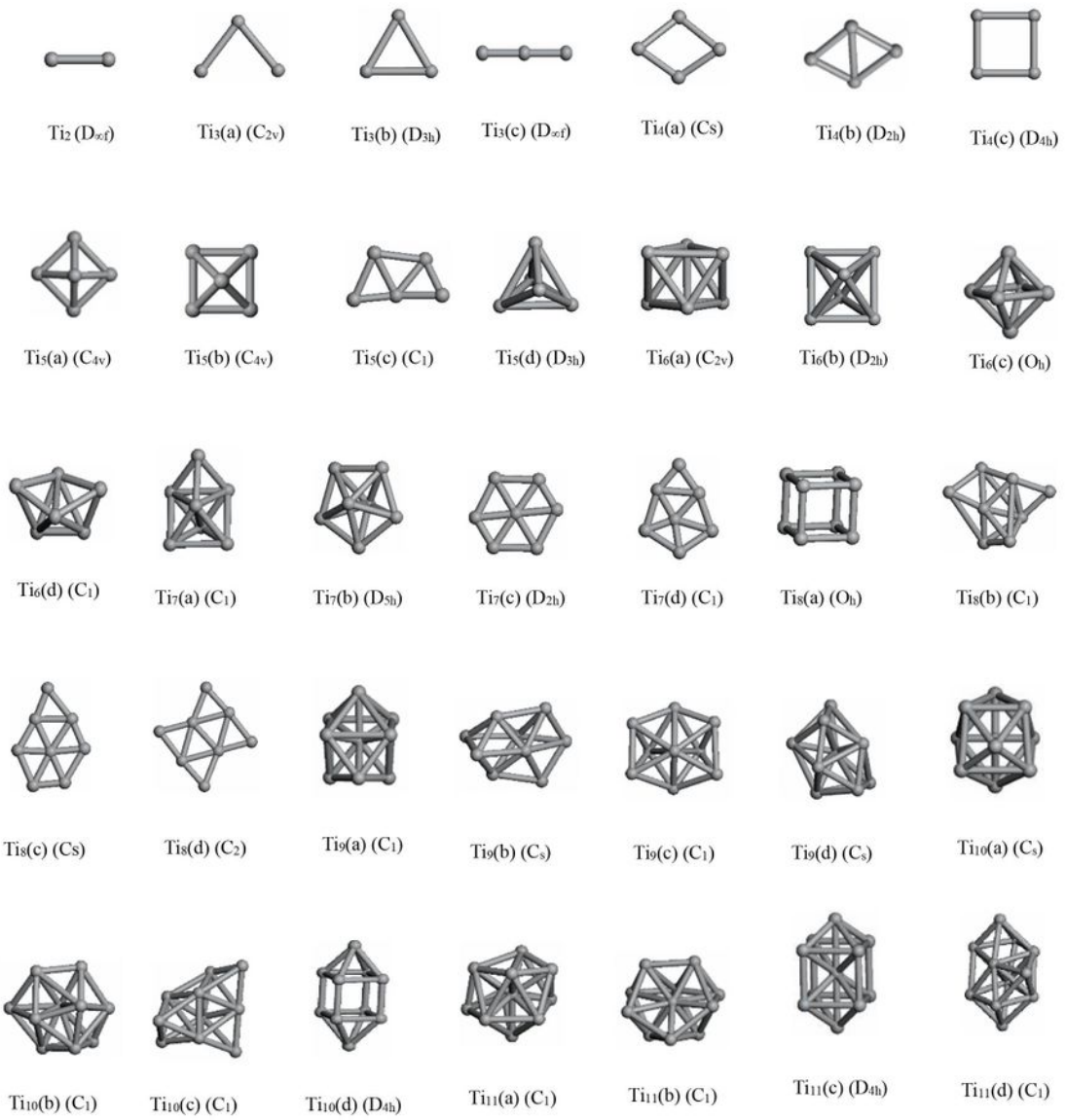

Fig.1

Figure 1

Optimized geometries of the lowest-energy sturctures with their isomers and the point group symmetry for Ti_{n+1} (n=1-10)

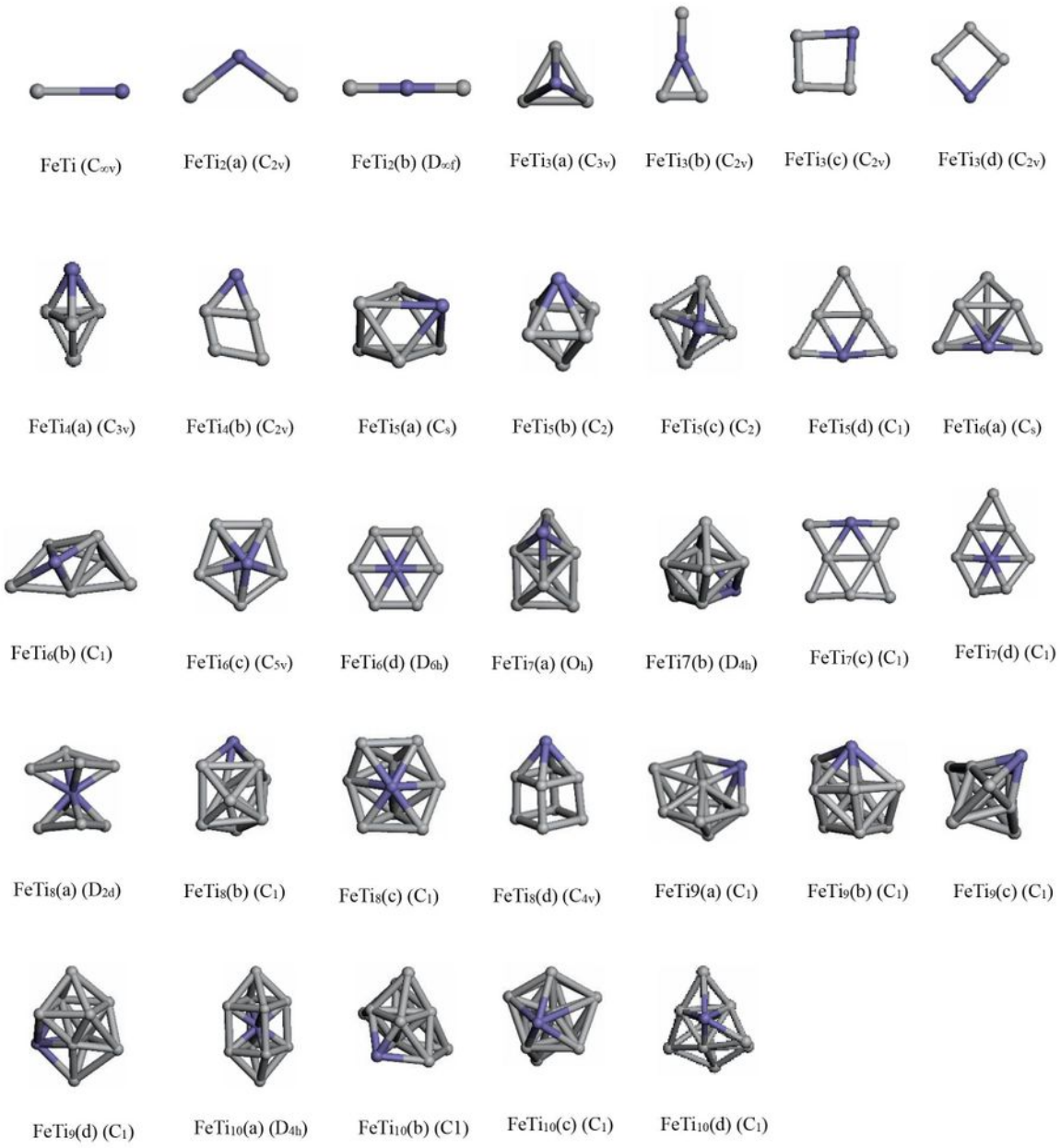

Fig.2

Figure 2

Optimized geometries of the lowest-energy sturctures with their isomers and the point group symmetry for $FeTi_n$ (n=1-10)

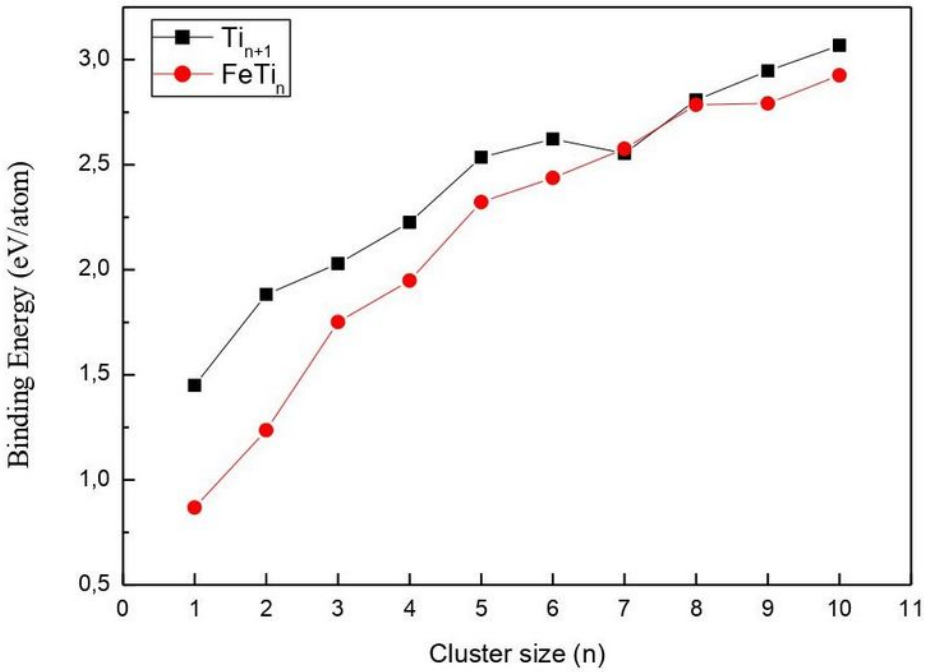

Fig. 3

Figure 3

Binding energy per atom (eV/atom) of Ti_{n+1} and $FeTi_n$ (n=1-10) clusters as a function of cluster size.

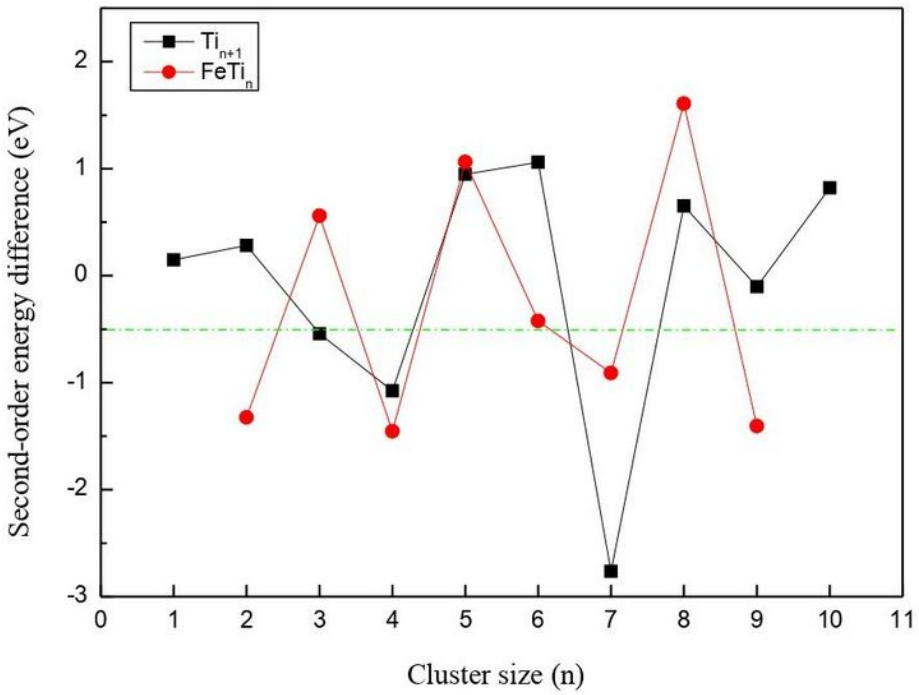

Fig.4

Figure 4

Second-order energy difference of Ti_{n+1} and $FeTi_n$ (n=1-10) clusters.

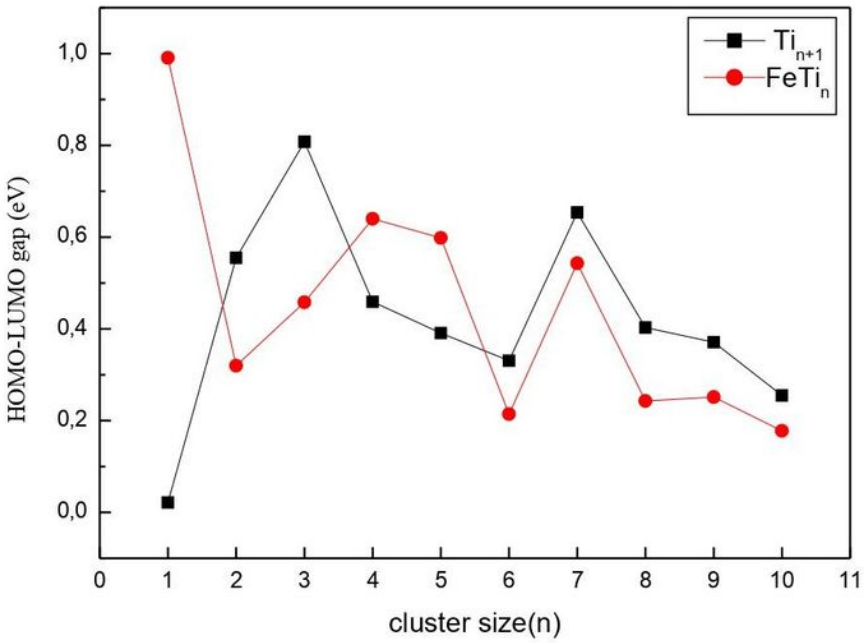

Fig.5

Figure 5

HOMO-LUMO gap Eg (eV) as a function of size for Ti_{n+1} and $FeTi_n$ (n=1-10) clusters.

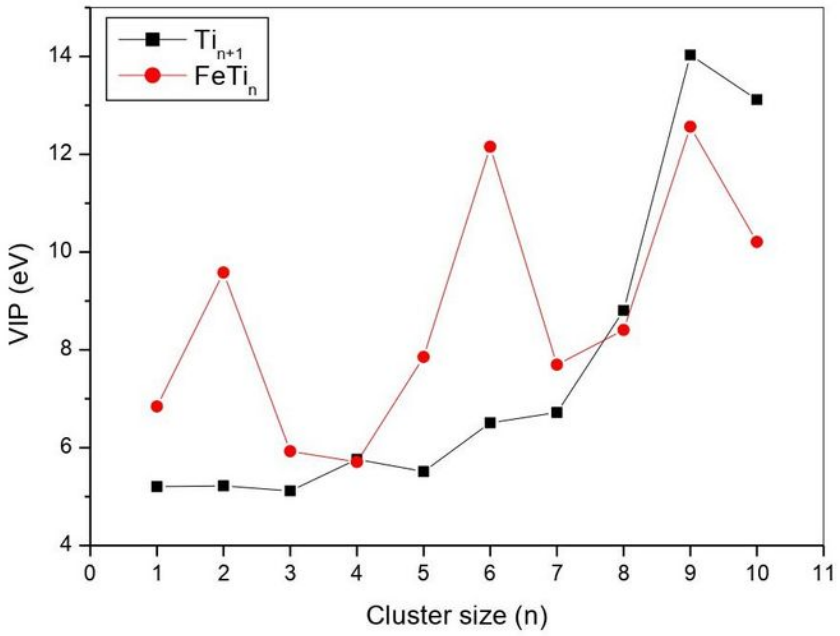

Fig.6

Figure 6

Vertical Ionization Potential (VIP) as a function of size for Ti_{n+1} and $FeTi_n$ (n=1-10) clusters.

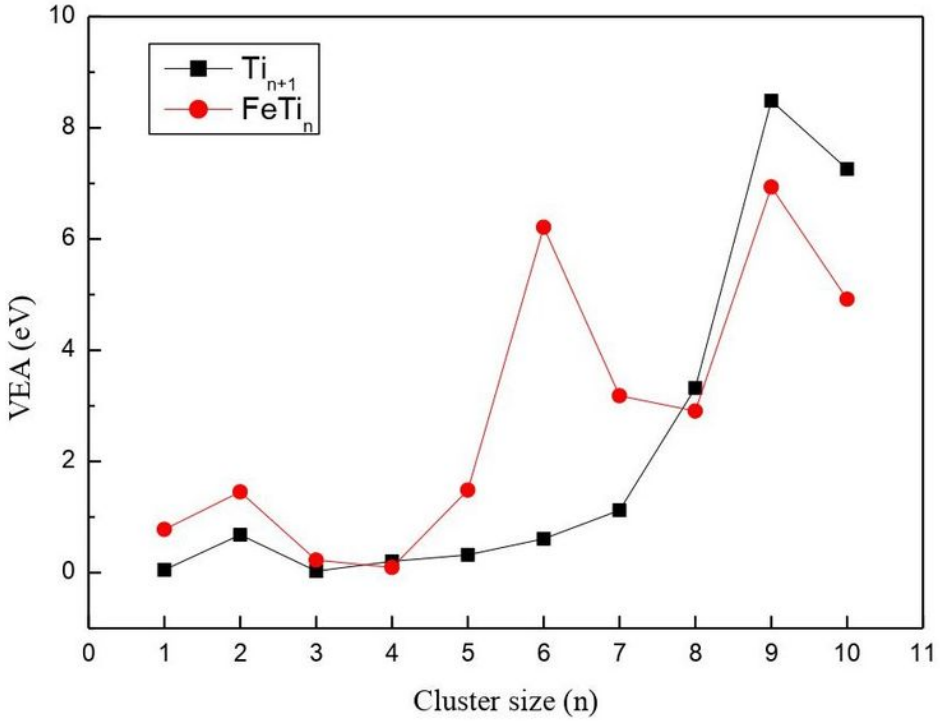

Fig.7

Figure 7

Vertical Electron Affinity (VEA) as a function of size for Ti_{n+1} and $FeTi_n$ (n=1-10) clusters.

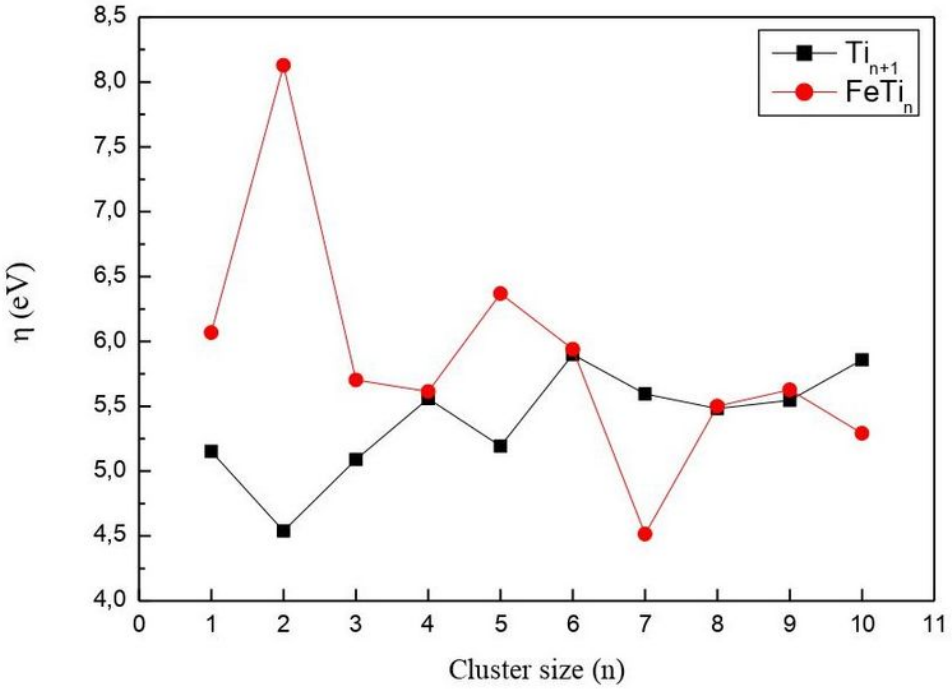

Fig.8

Figure 8

Chemical Hardness (η) as a function of cluster size for Ti_{n+1} and $FeTi_n$ (n=1-10) clusters.

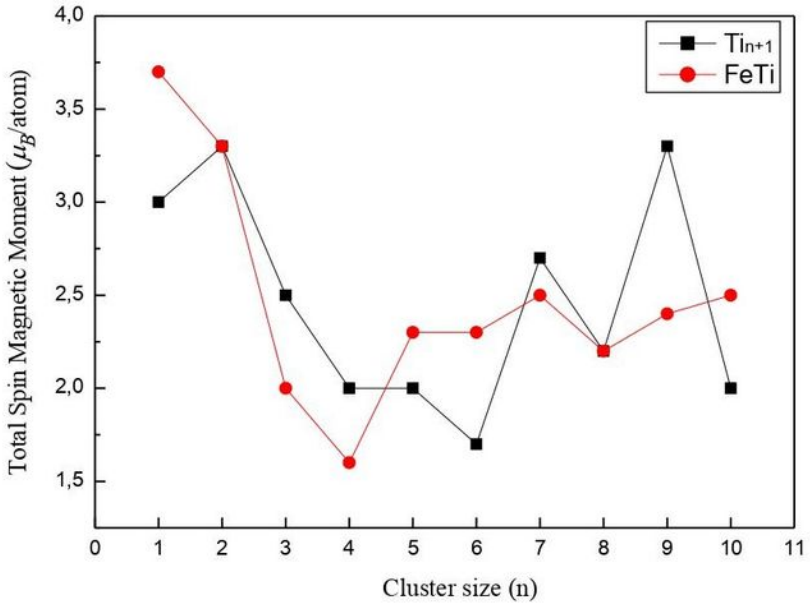

Fig.9

Figure 9

Average Spin Magnetic Moment (μB/atom) as a function of cluster size for Ti_{n+1} and $FeTi_n$ (n=1-10) clusters.

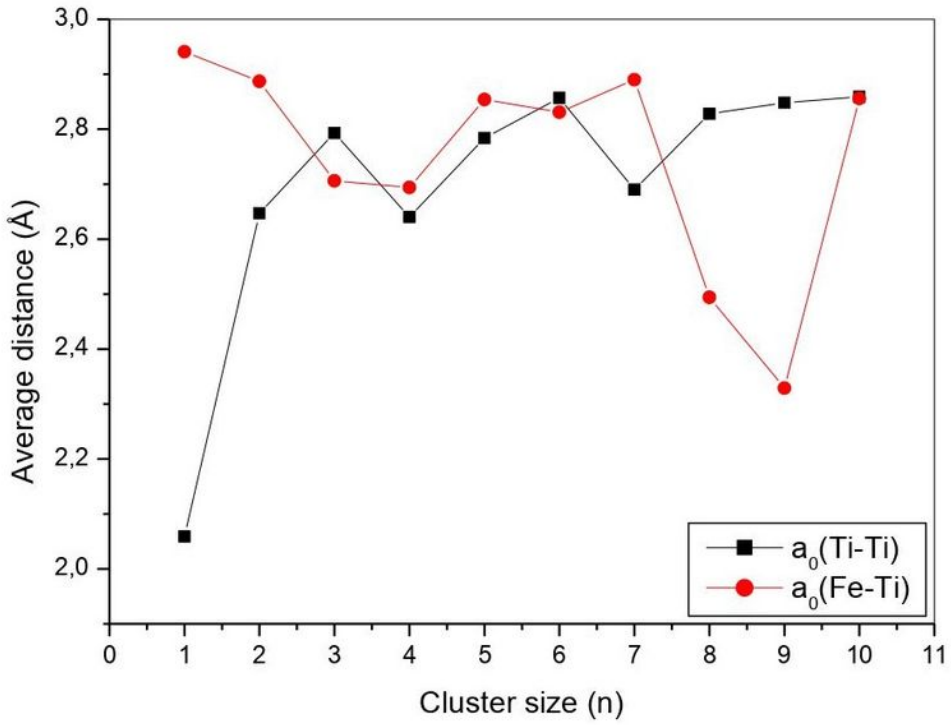

Fig.10

Figure 10

Average interatomic distances a0 (Ti-Ti) and a0 (Fe-Ti) as a function of cluster size for Ti_{n+1} and $FeTi_n$ (n=1-10) clusters.

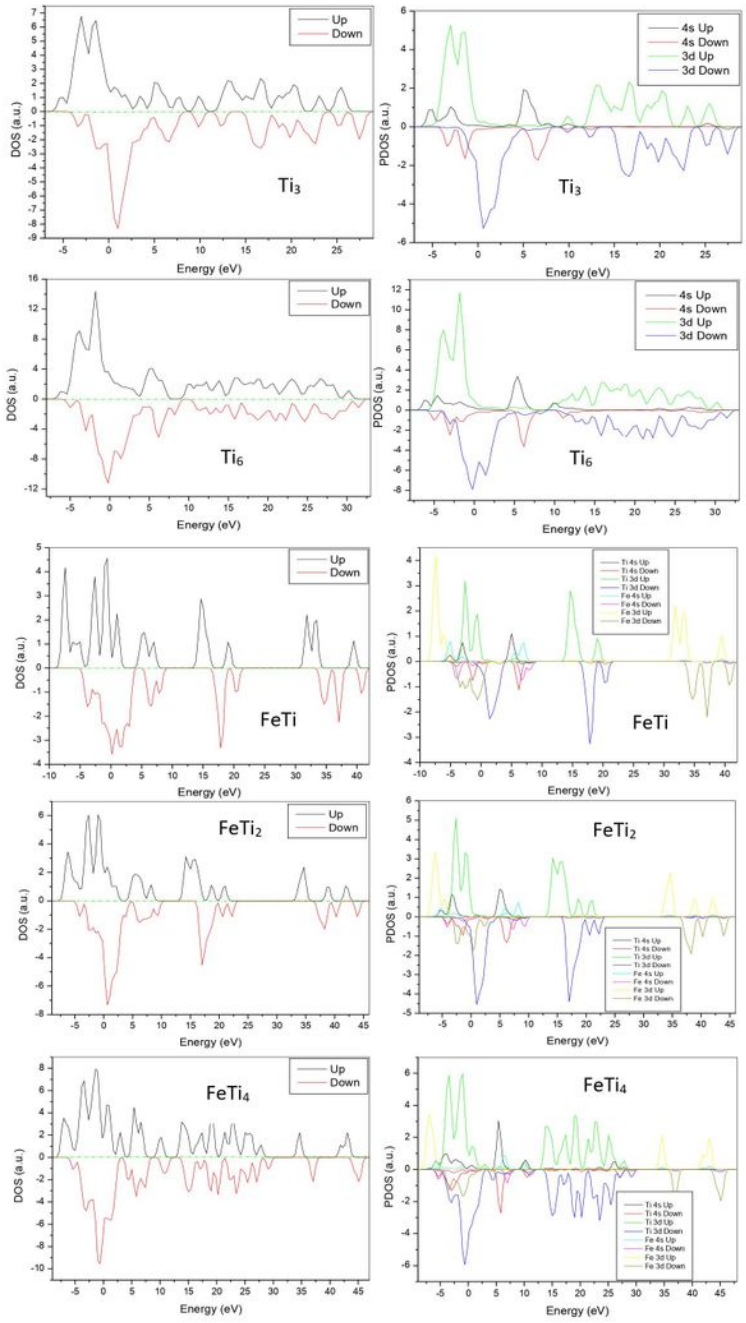

Fig.11

Figure 11

Total (DOS) and projected density of states (PDOS) for Ti_3, Ti_6, FeTi, $FeTi_2$, and $FeTi_4$ clusters.